ELSEVIER

Journal of Molecular Catalysis A: Chemical 118 (1997) 235–245

JOURNAL OF MOLECULAR CATALYSIS A: CHEMICAL

Time resolved FTIR study of the catalytic CO oxidation under periodic variation of the reactant concentration

J. Kritzenberger, A. Wokaun *

General Energy Research, Paul Scherrer Institute, CH-5232 Villigen PSI, and Department of Chemical Engineering and Industrial Chemistry, Swiss Federal Institute of Technology, ETH Zentrum, CH-8092 Zürich, Switzerland

Received 6 June 1996; accepted 5 September 1996

Abstract

Oxidation of CO over a palladium/zirconia catalyst obtained from an amorphous $Pd_{25}Zr_{75}$ precursor was investigated by time resolved FTIR spectroscopy. Sine wave shaped modulation of the reactant concentration, i.e., variation of CO or O_2 partial pressure, was used to induce dynamic variations of the IR signals of product (CO_2) and unconverted reactant (CO), which were detected in a multi-pass absorption cell. The phase shift, ϕ, between external perturbation and variation of the CO_2 signal was examined in dependence on temperature ($100 \leq T \leq 350$°C), partial pressure ($1 \times 10^{-4} \leq p_{CO}/p_{O_2} \leq 2$), and modulation frequency ($1.39 \times 10^{-4} \leq \omega \leq 6.67 \times 10^{-2}$ Hz). Comparison of modulation and step down experiments, performed by rapidly decreasing the CO inlet concentration, allows discrimination of parameter regimes characterized by different reaction orders. From the phase shift values, an Eley–Rideal mechanism is excluded, and the rate limiting step of the Langmuir–Hinshelwood mechanism for the CO oxidation may be identified. Adsorption and possible surface movement of CO to the actual reaction site determines the rate of the CO oxidation on the palladium/zirconia catalyst used in our study.

1. Introduction

The oxidation of carbon monoxide is of practical importance in exhaust treatment of combustion engines, and of fundamental interest in view of its kinetic behaviour. One may distinguish three characteristic zones of the reaction rate for CO oxidation over platinum or palladium catalysts as a function of both CO partial pressure and temperature. With increasing CO partial pressure the reaction rate first exhibits a linear increase, then an oscillating behaviour, and finally a quenched reaction state (reaction order -1 in CO) [1]. An analogous behaviour is reported for the reaction rate as a function of temperature. While at low temperature the CO oxidation rate over Pt, Pd, and Ir catalysts is of reaction order -1 in CO, it passes through a range of oscillation at increasing temperature, and exhibits a linear increase with CO partial pressure at higher temperatures [2]. On metal surfaces, the reaction proceeds via a Langmuir–Hinshelwood mechanism involving adsorbed CO and atomic oxygen [3–6]. Especially, the oscillating behaviour of the reaction rate was subject of intensive research efforts [1,2,7–10]. Periodic operation of the catalytic CO oxidation, which yields large increases of the reaction rate, is reviewed in [11].

* Corresponding author.

PII S1381-1169(96)00390-1

Novel preparation techniques have been used for the development of catalysts with a higher activity. For CO oxidation, highly active catalysts can be prepared from amorphous $Pd_{25}Zr_{75}$ alloys by controlled oxidation in air or by exposing the precursor to CO oxidation conditions [12,13]. In the activated form of the catalyst, oxygen is adsorbed on the substoichiometric zirconia, ZrO_{2-x}, and CO is adsorbed and oxidized on the surface of the palladium [14].

In this contribution, we describe a new approach for investigating the kinetics of catalytic reactions, using the example of CO oxidation over a catalyst prepared from an amorphous $Pd_{25}Zr_{75}$ precursor. The reaction order depending on CO partial pressure as well as temperature is deduced from reactant concentration modulation experiments; results are used to derive possible reaction paths. Time-resolved IR measurements are used to detect dynamic variations of IR signals induced by an external perturbation, i.e., by a sine wave shaped modulation of CO or O_2 partial pressure. The introduction of an external perturbation is a first step to the application of two dimensional infrared spectroscopy [15–17] to heterogeneously catalyzed reactions.

2. Experimental

The amorphous $Pd_{25}Zr_{75}$ alloy was kindly provided by A. Baiker. It was prepared by the melt spinning technique [18], and activated by exposing to CO oxidation conditions according to the procedure described in [19,20]. Catalytic experiments were performed in a continuous flow microreactor. A catalyst quantity of 164 mg was used in a glass reactor tube. The reactor was placed in a vertically mounted tube furnace (Carbolite) in which temperature was controlled within ± 0.5 K (Eurotherm controller).

The gas dosing system was designed to introduce up to three reaction gases independently into a flow of carrier gas. Gas flow was controlled by mass flow controllers (Bronkhorst, F201C) within ± 20 ml/min for the carrier gas N_2 and within ± 0.5 ml/min for the reaction gases CO and O_2, as well as for a second flow of nitrogen used to compensate each change in mass flows of the reaction gases. Due to limitation imposed by the specified range of the mass flow controllers (0.5–50 ml/min for the reaction gases and 20–2000 ml/min for the carrier gas), we used pure gases as well as gas mixtures. Nitrogen (99.999%), carbon monoxide (99.997%), oxygen (99.995%), and gas mixtures of carbon monoxide (99.997%): nitrogen (99.999%) = 1:10, 1:20 and 1:1000, were obtained from Carbagas (Rümlang, CH).

For detection of the infrared signals of products and unconverted reactants, we used a Bruker IFS55 FTIR spectrometer equipped with a multi-pass absorption cell (Infrared Analysis; pathlength: 3.2 m; volume: 120 ml). The rapid scan modus of the spectrometer enables to record a spectrum of 8 scans at 4 cm^{-1} resolution within 0.5 s.

Modulation experiments were performed as follows: The catalyst was held under reaction conditions for approximately 1 h, i.e., a continuous flow of N_2, O_2, and CO was passed through the reactor tube at the desired temperature. After recording the background spectrum (typically 1000 scans at 4 cm^{-1} resolution), a modulation experiment was started by varying the inlet mass flow of one reaction gas sinusoidally using the desired modulation frequency. Each change in the mass flow of the reaction gas was compensated by the opposite change in the N_2 (carrier gas) mass flow. Therefore, pressure and overall mass flow were constant during the experiments. Typical values of gas flows were 500 ml/min for N_2 and 1–40 ml/min for CO and O_2 and/or CO/N_2, O_2/N_2 gas mixtures. All experiments were performed using a constant overall mass flow of 530 ml/min, therefore pressure at the catalyst bed was constant during the experiments at approximately 3 bar.

After waiting at least 3 modulation periods to allow for adjustment of the system to the external perturbation, we started recording spectra by

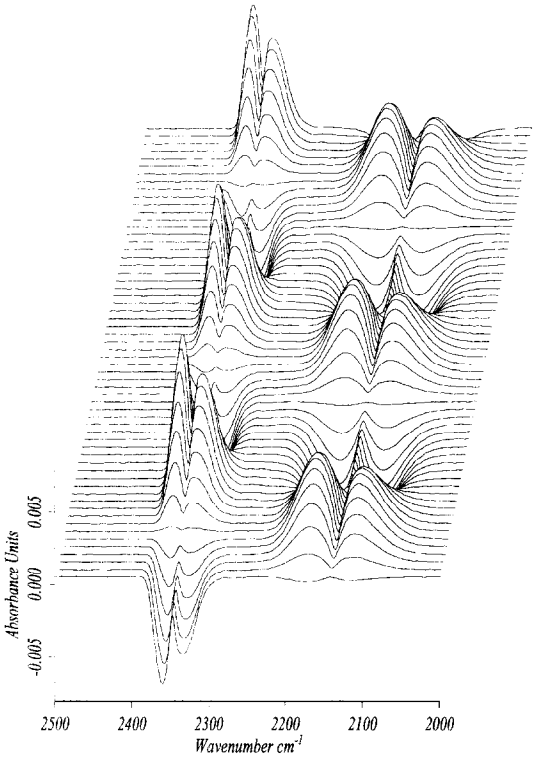

Fig. 1. Set of 60 spectra of a typical modulation experiment. Conditions for reference spectrum: $T = 180°C$; N_2: 485 ml/min, O_2: 5 ml/min, CO/N_2 (1/1000): 20 ml/min; N_2: 20 ml/min ($p_{CO}/p_{O_2} = 4 \times 10^{-3}$). Spectra were recorded during modulation of CO/N_2 gas mixture by a sine wave with a frequency of $\omega_{CO} = 3.33 \times 10^{-3}$ Hz (period 300 s) and an amplitude of 10 ml/min corresponding to partial pressure ration of $p_{CO}/p_{O_2} = 4 \times 10^{-3} \pm 2 \times 10^{-3}$. The nitrogen flow of 20 ml/min was modulated using the same frequency and amplitude but a 180° phase shift of the sine function. First trace (bottom) is recorded during the first 13.05 s after start of a modulation period, last trace is recorded after 770.9 to 784 s.

triggering the spectrometer at the starting time of the following modulation period. A set of 60 spectra was recorded during approximately 2 modulation periods. Typical values were 8 scans at 4 cm^{-1} resolution for a modulation period of 20 s and, e.g., 32 scans for a period of 60 s. A set of 60 spectra is shown in Fig. 1. The background spectrum (1000 scans, 4 cm^{-1} resolution) was recorded at $T = 180°C$ and constant gas flows of N_2: 485 ml/min, O_2: 5 ml/min, CO/N_2 (1/1000): 20 ml/min, and a secondary flow of N_2 of 20 ml/min. For recording the absorbance spectra (200 scans, 4 cm^{-1} resolution), the flow of the CO/N_2 gas mixture was modulated by a sine wave with a frequency of $\omega_{CO} = 3.33 \times 10^{-3}$ Hz (period 300 s) and an amplitude of 10 ml/min. The change in the overall gas flow was compensated by modulating the N_2 flow of 20 ml/min in the same manner as for CO/N_2 but with a 180° phase shift. The first trace in Fig. 1 (bottom) is recorded during the first 13.05 s after start of a modulation period, the last trace is recorded after 770.9 to 784.0 s. The phase shift, ϕ, between the CO signal (around 2150 cm^{-1}) and the CO_2 signal (around 2350 cm^{-1}) is deduced by determining the arithmetic average of one phase shift of peak maxima and one phase shift of peak minima. Examination of a contour plot of the spectra is a convenient way to determine ϕ.

Modulation frequency limits of $\omega = 1.39 \times 10^{-4}$ Hz (corresponding to a period of 2 h) and $\omega = 6.67 \times 10^{-2}$ Hz (corresponding to a period of 15 s) were given by the experimental setup. The lower limit was caused by the instability of the background, the upper limit by the tube volume of approximately 18 ml between mass flow controllers and multi pass gas cell. With increasing modulation frequency, the periodic changes in the reactant partial pressure were levelled by this dead volume.

CO step down experiments were performed starting with the maximum partial pressure ratio of p_{CO}/p_{O_2}, of the corresponding modulation experiment. These conditions were used to record the background spectrum (typically 1000 scans at 4 cm^{-1} resolution). Detection of the absorbance spectra was started at the time the CO inlet concentration was lowered to the minimum value of the modulation experiment. For a modulation experiment performed using $p_{CO}/p_{O_2} = 3.125 \times 10^{-3} \pm 1.25 \times 10^{-3}$ the corresponding step down experiment was performed starting at a $p_{CO}/p_{O_2} = 4.375 \times 10^{-3}$ followed by a decrease to $p_{CO}/p_{O_2} = 1.875 \times 10^{-3}$. Each change in the CO mass flow was compensated by the inverse change in the N_2 mass flow. Fig. 2 shows the sequence of gas

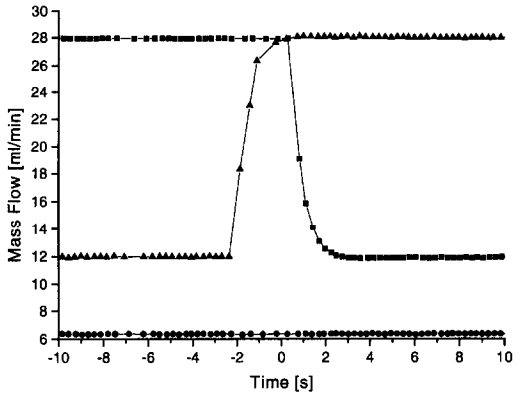

Fig. 2. Gas flows during the step down experiment at $T = 180°C$ performed by lowering P_{CO}/p_{O_2} from 4.375×10^{-3} to 1.875×10^{-3}. Inlet concentrations were recorded by the mass flow controllers for $CO/N_2 = 1/1000$ (–■–), O_2 (–·–), and N_2 (–▲–). The corresponding CO_2 concentration, as determined by integration of the IR signal detected in the multi-pass gas cell, is included in Fig. 3. The starting time of recording spectra is set to 0.

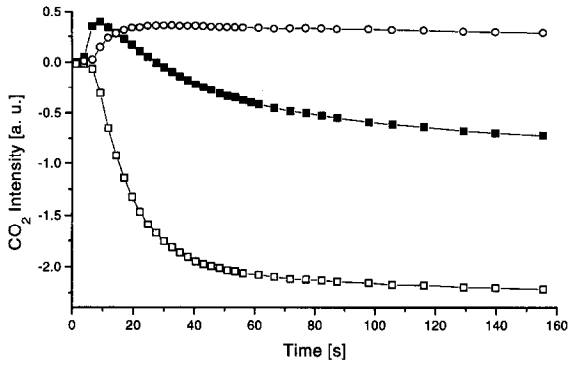

Fig. 3. Step down experiments at $T = 150°C$ (–○–), $T = 180°C$ (–■–), and $T = 240°C$ (–□–). Intensity of the CO_2 peak is integrated between 2282 and 2389 cm^{-1}. Reference conditions: N_2: 483.6 ml/min; O_2: 6.4 ml/min; CO/N_2 (1/1000): 28 ml/min; N_2: 12 ml/min. Spectra were recorded after switching gas flows: CO/N_2 (1/1000): 28 ml/min → 12 ml/min; N_2: 12 ml/min → 28 ml/min. The changes in gas flows correspond to a decrease of the partial pressure ratio p_{CO}/p_{O_2} from 4.375×10^{-3} to 1.875×10^{-3}.

flow changes during a step down experiment recorded as inlet concentration by the mass flow controllers, and defines the starting time of spectra detection.

3. Results

3.1. Temperature dependence of carbon monoxide step down and modulation experiments

Step down experiments were performed at $T = 150$, 180, and 240°C by decreasing the p_{CO}/p_{O_2} ratio of the inlet partial pressure from 4.375×10^{-3} to 1.875×10^{3}. The integrated absorbance of the CO_2 signal (referenced versus the spectrum recorded at starting conditions) is shown in Fig. 3. For $T = 150°C$ (Fig. 3: –○–) the reduction of CO concentration is followed by an increase of the CO_2 concentration which indicates a reaction order of -1 in CO. At $T = 180°C$ (Fig. 3: –■–) the response of the system under the same experimental conditions is an initial increase of the CO_2 concentration, followed by an exponential decrease. Approximately 30 s after the step down of the CO concentration the absorbance of CO_2 reaches the initial value which is reflected by an absorbance change of 0. Further increase of the temperature to $T = 240°C$ (Fig. 3: –□–) yields an exponential decay of the CO_2 product partial pressure after the step.

Modulation experiments were performed using two different modulation frequencies, i.e., 1.66×10^{-2} Hz and 4×10^{-2} Hz corresponding to periods of 60 and 25 s, respectively. Fig. 4 shows the phase shift of the CO_2 signal relative to the phase of the external perturbation

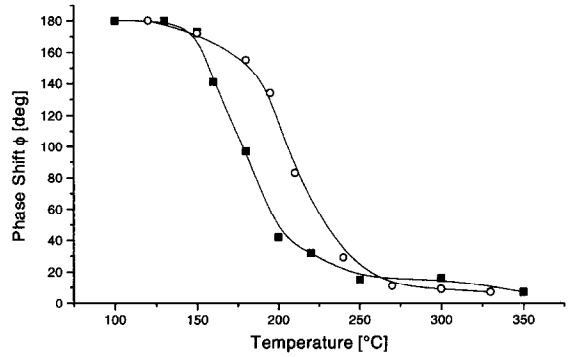

Fig. 4. Phase shift ϕ between the CO_2 signal and the CO signal versus T for modulation frequencies $\omega_{CO} = 1.67 \times 10^{-2}$ Hz (–■–; period 60 s) and $\omega_{CO} = 4 \times 10^{-2}$ Hz (–○–; period 25 s). Spectra were recorded during modulation of $p_{CO}/p_{O_2} = 3.125 \times 10^{-3} \pm 1.25 \times 10^{-3}$ at a constant overall mass flow of 530 ml/min and referenced versus a reference spectrum recorded using $p_{CO}/p_{O_2} = 3.125 \times 10^{-3}$.

of the system, performed as cyclic variation of the CO inlet concentration compensated by a 180° phase shifted nitrogen variation as described in the experimental section. In Fig. 4, three different regions of ϕ values can be separated.

For $T \leq 150$°C, the system responds with a phase shift $\phi = 180°$ of the CO_2 signal. Obviously a 180° phase shift of CO_2 relative to CO characterizes the inverse reaction zone, in which a higher CO inlet concentration yields a lower CO_2 production and reverse. This corresponds to the step down experiments for $T \leq 150$°C which show an increase of the CO_2 production. Note that 180° phase shift holds for both modulation frequencies.

For $T \geq 240$°C, a phase shift $\phi < 30°$ is detected which becomes gradually smaller with increasing temperature. Step down experiments in the corresponding temperature region show an exponential decay of the CO_2 concentration after lowering the CO inlet concentration. Therefore a phase shift of $\phi < 30°$ reflects the area of reaction order 1 in CO, i.e., the more CO is available the more CO_2 is produced. Note the similar phase shifts for both modulation frequencies.

For intermediate temperatures, a strong dependence of ϕ on T is detected. The phase shift decreases starting at $\phi = 180°$ ($T = 130$°C) to $\phi \approx 30°$ ($T = 240$°C). In this region, ϕ depends on the modulation frequency, i.e., at the same temperature a modulation period of 25 s yields a higher value of ϕ compared to a modulation period of 60 s. Comparison of the phase shift values at $T = 180$°C ($\phi = 155°$ for $\omega = 4 \times 10^{-2}$ Hz; $\phi = 97°$ for $\omega = 1.66 \times 10^{-2}$ Hz) with the corresponding step down experiment explains the reason for this behaviour. Approximately 30 s after the initial increase of the CO_2 production in the step down experiments, the CO_2 concentration reaches the initial value. For a modulation frequency of 4×10^{2} Hz, this means that a full modulation period is completed within the time window of increased CO_2 concentration. As explained above, an increased CO_2 value reflects a reaction order of -1 in CO which again is characterized by a phase shift of $\phi = 180°$. Consequently a modulation period of 25 s detects mainly the inverse reaction regime and therefore shows a phase shift close to 180°. In contrast, a modulation period of 60 s detects approximately equal contributions of inverse and linear reaction behaviour, as reflected in a phase shift $\phi = 90°$.

3.2. Partial pressure dependence of carbon monoxide step down and modulation experiments

The integrated intensity of the CO_2 peak in step down experiments performed at $T = 180$°C is shown in Fig. 5 for changes in the mean partial pressure ratio p_{CO}/p_{O_2} of 2 (–○–), 3.3×10^{-4} (–■–), and 1×10^{-4} (–□–). For a mean partial pressure ratio chnage of 2, the

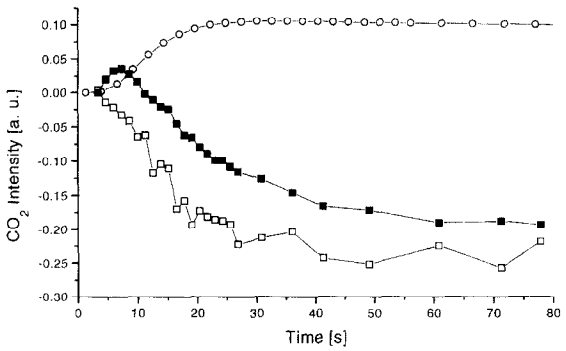

Fig. 5. Step down experiments at different partial pressure ratios p_{CO}/p_{O_2} ($T = 180$°C). Intensity of the CO_2 peak is integrated between 2282 cm^{-1} and 2389 cm^{-1}. Upper trace (–○–): Reference conditions: N_2: 525 ml/min; O_2: 1 ml/min; CO: 3 ml/min; N_2: 1 ml/min. Spectra were recorded after switching gas flows: CO: 3 ml/min → 1 ml/min, N_2: 1 ml/min → 3 ml/min. The changes in gas flows correspond to a decrease of the partial pressure ratio p_{CO}/p_{O_2} from 3 to 1. Middle trace (–■–): reference conditions: N_2: 480 ml/min; O_2: 30 ml/min; CO/N_2 (1/1000): 15 ml/min; N_2: 525 ml/min. Spectra were recorded after switching gas flows: CO/N_2 (1/1000): 15 ml/min → 5 ml/min; N_2: 5 ml/min → 15 ml/min (decrease in partial pressure ratio p_{CO}/p_{O_2} from 5×10^{-4} to 1.67×10^{-4}). Lower trace (–□–): Reference conditions: N_2: 482 ml/min; O_2: 40 ml/min; CO/N_2 (1/1000): 7 ml/min; N_2: 1 ml/min. Spectra were recorded after switching gas flows: CO/N_2 (1/1000): 7 ml/min → 1 ml/min; N_2: 1 ml/min → 7 ml/min (decrease in partial pressure ratio p_{CO}/p_{O_2} from 1.75×10^{-4} to 2.5×10^{-5}).

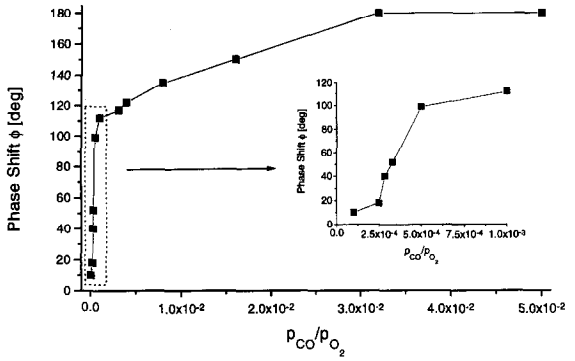

Fig. 6. Phase shift ϕ between the CO_2 signal and the CO signal versus p_{CO}/p_{O_2} (x_0) for a modulation frequency $\omega_{CO} = 2.5 \times 10^{-2}$ Hz (period 40 s) at $T = 180°C$. Spectra were recorded during modulation of $P_{CO}/p_{O_2} \approx x_0 \pm (x_0/4)$ at a constant overall mass flow of 530 ml/min and referenced versus a background spectrum recorded using $p_{CO}/p_{O_2} = x_0$.

step down in the CO inlet concentration is followed by an increase of the CO_2 concentration which is the characteristic behaviour of the inverse reaction regime. A step down experiment at a comparably lower partial pressure ratio yields an exponential decrease of the CO_2 concentration reflecting the area of reaction order 1 in CO. For intermediate partial pressure ratios, an initial increase of the CO_2 production is followed by an exponential decrease of the outlet concentration.

The phase shift, ϕ, between the CO_2 signal and the CO signal determined in modulation experiments performed using a modulation frequency of 2.5×10^{-2} Hz (40 s period), is shown in Fig. 6. As was found in the study of temperature dependence, the inverse reaction regime is characterized by a phase shift of 180°. For a 40 s modulation period, $\phi = 180°$ is reached for partial pressure ratios of and above 3.2×10^{-2}.

In step down experiments, an exponential decrease of the CO_2 concentration without initial increase is detected for partial pressure ratios of 2.5×10^{-4} and smaller. The corresponding modulation experiment at $p_{CO}/p_{O_2} = 2.5 \times 10^{-4}$ yields a value of $\phi = 18°$. Therefore, the linear reaction regime is characterized by a phase shift $\phi < 20°$.

As mentioned, the phase shift of the CO_2 signal relative to the CO signal shows a strong dependence on the p_{CO}/p_{O_2} partial pressure ratio for $3.2 \times 10^{-2} > p_{CO}/p_{O_2} > 2.5 \times 10^{-4}$ (Fig. 6). Comparison with the step down experiments performed at average values of $p_{CO}/p_{O_2} = 3.125 \times 10^{-3}$ ($T = 180°C$; Fig. 3) and $p_{CO}/p_{O_2} = 3.33 \times 10^{-4}$ ($T = 180°C$; Fig. 5) can explain this dependence. The step down experiment performed at $p_{CO}/p_{O_2} = 3.33 \times 10^{-4}$ shows an initial increase of the CO_2 concentration which reaches the initial value after approximately 12 s. Therefore, a modulation period of 40 s will sample, for more than half of the period, the linear reaction area which yields a shift $\phi < 90°$ ($\phi = 52°$).

The step down experiment performed at $p_{CO}/p_{O_2} = 3.125 \times 10^{-3}$ (Fig. 3) shows an increase of the CO_2 concentration which reaches the initial value after approximately 30 s. In the corresponding modulation experiment at $\omega = 2.5 \times 10^{-2}$ Hz, more than half of the period corresponds to the inverse reaction regime which yields a shift value of $\phi > 90°$ ($\phi = 117°$).

3.3. Modulation frequency dependence

Interpretation of the $\phi(\omega)$ data as a function of both temperature and partial pressure calls for a model for the dependence of the phase shift, ϕ, on the modulation frequency, ω. The corresponding experiments for a modulation of $p_{CO}/p_{O_2} = 4 \times 10^{-3} \pm 2 \times 10^{-3}$ performed by varying the CO partial pressure at $T = 180°C$ are shown in Fig. 7. The limits of the modulation frequency used are given by the experimental setup as described in the experimental section.

For a qualitative explanation, we compare the values of ϕ with the step down experiment performed at $T = 180°C$ and comparable partial pressure ratio ($p_{CO}/p_{O_2} = 4.375 \times 10^{-3} \rightarrow 1.875 \times 10^{-3}$; Fig. 3; –■–). In the step down experiment the system responds with an increase of the CO_2 production after a decrease of the CO inlet concentration followed by an exponential decay of the CO_2 partial pressure.

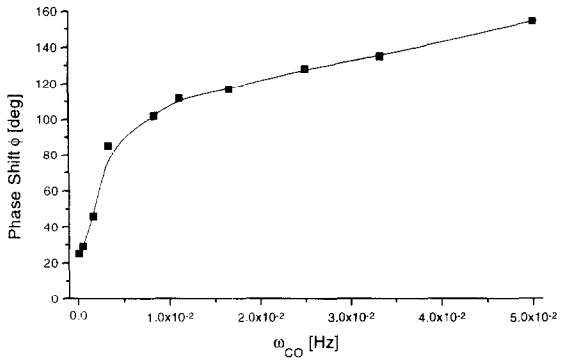

Fig. 7. Phase shift ϕ between the CO_2 signal and the CO signal for different modulation frequencies ω_{CO} at $T = 180°C$. Spectra were recorded during modulation of $p_{CO}/p_{O_2} = 4 \times 10^{-3} \pm 2 \times 10^{-3}$ at a constant overall mass flow of 530 ml/min and referenced versus a background spectrum recorded using $p_{CO}/p_{O_2} = 4 \times 10^{-3}$.

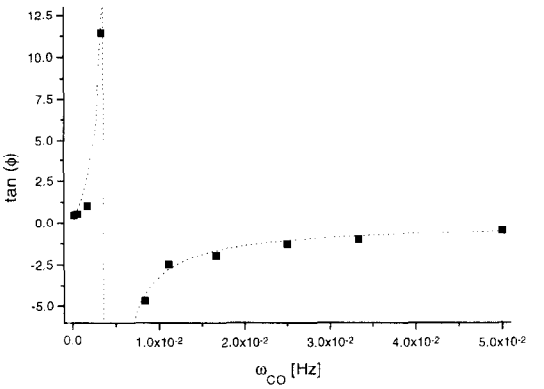

Fig. 8. Simulation of the modulation experiment using $p_{CO}/p_{O_2} = 4 \times 10^{-3} \pm 2 \times 10^{-3}$ (for experimental conditions see caption of Fig. 7. Fit of tan(ϕ) versus ω_{CO} using Eq. (2) yields $\omega_0 = (4.3 \pm 0.2) \times 10^{-3}$ Hz and $\tau = 77$ s.

Therefore, for short modulation periods (corresponding to high frequency values), we detect a shift value close to 180° which characterizes the regime of reaction order −1 in CO. Lowering the modulation frequency corresponds to an increasing contribution of the decaying part detected by the modulation experiment, which is reflected in decreasing shift values.

In classical physics, similar curves for the dependence of phase shift on the modulation frequency are encountered for forced vibrations of a damped harmonic oscillator. Solution of the differential equation

$$m\frac{d^2x}{dt^2} + r\frac{dx}{dt} + kx = K_0 e^{i\omega t} \quad (1)$$

yield

$$\tan(\phi) = \frac{r}{m}\frac{\omega}{\omega_0^2 - \omega^2} \quad (2)$$

with phase shift ϕ, modulation frequency ω, eigenfrequency of the oscillator ω_0, oscillator parameters m, r, k, and modulation amplitude K_0. The quantity (r/m) determines the lifetime τ according to

$$\tau = 2\frac{m}{r} \quad (3)$$

Fig. 8 shows a plot of tan(ϕ) versus ω_{CO} for a modulation experiment using $p_{CO}/p_{O_2} = 4 \times 10^{-3} \pm 2 \times 10^{-3}$ ($T = 180°C$). A fit of these values using Eq. (2) yields an eigenfrequency $\omega_0 = (4.3 \pm 0.2) \times 10^{-3}$ Hz and a lifetime $\tau = 77$ s. The eigenfrequency, ω_0, may be associated with an overall rate constant, and will be used as a characteristic value to compare the velocity of the CO oxidation under different p_{CO}/p_{O_2} partial pressure ratios.

Fig. 9 shows experimental values, and the corresponding fit of tan(ϕ) versus ω_{CO} using Eq. (2), for a modulation experiment performed at $p_{CO}/p_{O_2} = 3.33 \times 10^{-4} \pm 1.66 \times 10^{-4}$ ($T =$

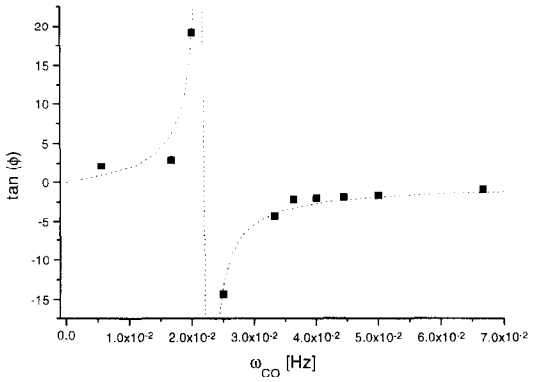

Fig. 9. Simulation of the modulation experiment using $p_{CO}/p_{O_2} = 3.33 \times 10^{-4} \pm 1.67 \times 10^{-4}$. Fit of tan($\phi$) versus ω_{CO} using Eq. (2) yields $\omega_0 = (2.20 \pm 0.03) \times 10^{-2}$ Hz and $\tau = 27$ s. Spectra were recorded during modulation of $p_{CO}/p_{O_2} = 3.33 \times 10^{-4} \pm 1.67 \times 10^{-4}$ at a constant overall mass flow of 530 ml/min (T = 180°C) and referenced versus a background spectrum recorded using $p_{CO}/p_{O_2} = 3.33 \times 10^{-4}$.

180°C). The fit yields an eigenfrequency of $(2.20 \pm 0.03) \times 10^{-2}$ Hz and a lifetime $\tau = 27$ s. Thus, with decreasing partial pressure ratio p_{CO}/p_{O_2} the system is shifted towards the linear reaction regime, and therefore one expects an increasing reaction rate.

In order to characterize the regime of reaction order 1 in CO, the values of ϕ as a function of ω_{CO} were detected at $p_{CO}/p_{O_2} = 1 \times 10^{-4} \pm 0.75 \times 10^{-4}$ ($T = 180$°C). For the medium partial pressure ratio the step down experiment (Fig. 5) shows an exponential decrease without any initial increase of the CO_2 partial pressure. In Fig. 10 the phase shift ϕ of the CO_2 signal is plotted versus ω_{CO}. Within the experimental limits, ϕ is varying between 13° ($\omega = 5.56 \times 10^{-3}$ Hz) and 35° ($\omega = 5 \times 10^{-2}$ Hz). Obviously, the characteristic frequency value belonging to a phase shift of 90° is outside of our experimental frequency window. From the shift values, we can deduce an overall rate constant for the reaction order 1 in CO of more than 5×10^{-2} s^{-1}.

In Fig. 10, two additional shift values recorded at $p_{CO}/p_{O_2} = 3.125 \times 10^{-3} \pm 1.25 \times 10^{-3}$ and $T = 240$°C are plotted. At this comparable high partial pressure ratio, an increase in temperature to 240°C yields similar shift values as the experiment performed at $T = 180$°C and $p_{CO}/p_{O_2} = 1 \times 10^{-4} \pm 0.75 \times 10^{-4}$. These values once again show the similarity of the system response for decreasing p_{CO}/p_{O_2} partial pressure ratio and increasing temperature. With both experimental parameters, one can reach the area of reaction order 1 in CO.

In addition, values $\phi(\omega_{CO})$ were recorded at $p_{CO}/p_{O_2} = 4 \times 10^{-2} \pm 0.5 \times 10^{-2}$ ($T = 180$°C) in order to characterize the regime of reaction order -1 in CO. Within the experimental bandwidth of the modulation frequency we detect a phase shift of 180° for each value of ω_{CO}. As mentioned, a phase shift of 180° is characteristic for the area of inverse reaction order in contrast to a value close to 0° for the area of reaction order 1 in CO. Therefore a value of $\phi = 180$° independent of modulation frequency indicates that all frequencies used in our experiments are too low for detecting the additional shift values that would be characteristic for competition between CO and O_2 for adsorption sites (see Discussion). We conclude a rate constant higher than 5×10^{-2} s^{-1} for the latter reaction.

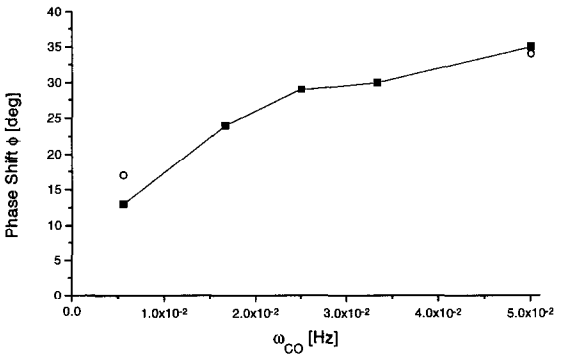

Fig. 10. Phase shift ϕ between the CO_2 signal and the CO signal for different modulation frequencies ω_{CO}. The overall mass flow was constant (530 ml/min) during the experiments. For values plotted as (–■–) spectra were recorded during modulation of $p_{CO}/p_{O_2} = 1.10 \times 10^{-4} \pm 0.75 \times 10^{-4}$ at $T = 180$°C and referenced versus a background spectrum recorded using $p_{CO}/p_{O_2} = 1 \times 10^{-4}$. For values plotted as (O) spectra were recorded during modulation of $p_{CO}/P_{O_2} = 3.125 \times 10^{-3} \pm 1.25 \times 10^{-3}$ at $T = 240$°C and referenced versus a background spectrum recorded using $p_{CO}/P_{O_2} = 3.125 \times 10^{-3}$.

3.4. Oxygen modulation experiments

As reported for the CO modulation, we have performed temperature dependent, partial pressure dependent, and modulation frequency dependent measurements of the phase shift ϕ of the CO_2 signal relative to modulation of the O_2 partial pressure. Due to the fact that O_2 does not show a detectable IR-signal, the uncertainty in the shift values is significantly higher compared to the CO modulation experiments. Nevertheless, from the CO experiments the phase of detection in the IR-spectrometer relative to external perturbation as introduced by the mass flow controllers is well known.

Experiments were performed in the temperature range between 130 and 350°C ($P_{CO}/p_{O_2} = 3.125 \times 10^{-3} \pm 1.25 \times 10^{-3}$; $\omega_{O_2} = 1.66 \times 10^{-2}$ Hz), for partial pressure ratios between

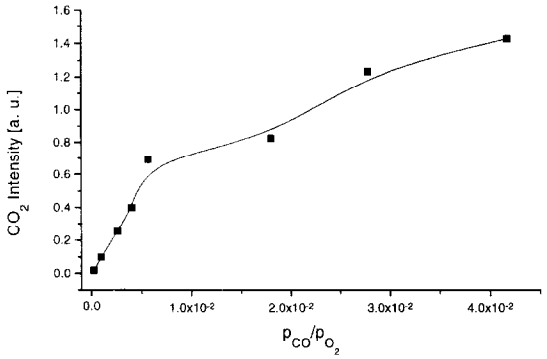

Fig. 11. Oxygen modulation experiments performed using $\omega_{O_2} = 2.5 \times 10^{-2}$ Hz (period 40 s) and $T = 180$°C. The overall mass flow was constant (530 ml/min) during the experiments. Spectra were recorded during modulation of the oxygen mass flow using a constant modulation amplitude of ±2 ml/min and referenced versus a background spectrum recorded using the average O_2 mass flow.

$P_{CO}/p_{O_2} = 2.5 \times 10^{-4}$ and $p_{CO}/p_{O_2} = 4.167 \times 10^{-2}$ ($T = 180$°C; $\omega_{O_2} = 2.5 \times 10^{-2}$ Hz), and modulation frequencies between $\omega_{O_2} = 8.33 \times 10^{-3}$ and 5×10^{-2} Hz ($T = 160$°C; $p_{CO}/p_{O_2} = 0.15625$). In all experiments, there was no detectable phase shift between the external perturbation (modulation of the O_2 inlet partial pressure) and the CO_2 signal, i.e., $\phi = 0$. These results show that the CO_2 production follows immediately (within the experimental limits) any change in the O_2 concentration.

In contrast to the phase shift, ϕ, which is independent from partial pressure, there is a strong dependence of the *amount* of CO_2 produced on p_{CO}/p_{O_2} when modulating the O_2 reactant concentration. The experiments were performed at $T = 180$°C and $\omega_{O_2} = 2.5 \times 10^{-2}$ Hz with a constant modulation amplitude of O_2, i.e., in each experiment the mass flow of O_2 was modulated by ±2 ml/min. In Fig. 11, the change in the integrated absorbance of CO_2 is plotted versus p_{CO}/p_{O_2}. For the area of reaction order 1 in CO (lowest p_{CO}/p_{O_2} value shown in Fig. 11) there is no detectable change in the CO_2 concentration when varying the O_2 mass flow. This is in agreement with reaction order 0 in O_2 reported in Ref. [1]. With increasing partial pressure ratio P_{CO}/p_{O_2} the modulation amplitude of the CO_2 concentration increases (at a constant O_2 mass flow modulation of ±2 ml/min). This behaviour corresponds to a reaction order in O_2 increasing from 0 to 1 [1].

4. Discussion

Comparison of step down and modulation experiments leads to characteristic phase shift values of $\phi = 180°$ for the area of reaction order −1 in CO and $\phi < 30°$ for the regime of reaction order 1 in CO. The inverse reaction area can be reached either by reducing temperature to $T \leq 120$°C at $p_{CO}/p_{O_2} = 3.125 \times 10^{-3}$, or by increasing the partial pressure ratio P_{CO}/p_{O_2} to $\geq 3.2 \times 10^{-2}$ at $T = 180$°C. The zone of reaction order 1 in CO can be reached either by increasing temperature to $T \geq 240$°C at $p_{CO}/p_{O_2} = 3.125 \times 10^{-3}$, or by reducing the partial pressure ratio p_{CO}/p_{O_2} to $\leq 1 \times 10^{-4}$ at $T = 180$°C. In the oscillation region ϕ exhibits a strong dependence on temperature T, partial pressure ratio p_{CO}/p_{O_2}, and modulation frequency to ω_{CO}. These experiments show that the phase shift, ϕ, induced by an external perturbation is a unique value characterizing the oxidation of carbon monoxide performed at a defined set of experimental conditions (T, p_{CO}/p_{O_2}, ω_{CO}).

As possible reaction paths for the CO oxidation, Fig. 12 shows schematically the Eley–Rideal (upper scheme) and the Langmuir–Hinshelwood (lower scheme) mechanism. Supposing the validity of the Eley–Rideal mechanism an increasing O_2 partial pressure should result in an increasing or at least a constant CO_2 production even at high p_{CO} values. The observed phase shift of 180° independent of ω_{CO} for $p_{CO}/p_{O_2} \geq 3.2 \times 10^{-2}$ is in contradiction to the Eley–Rideal mechanism. Taking into account that the modulation amplitude of CO_2 production increases with CO partial pressure (Fig. 11), the only possible explanation for the existence of a negative power dependence is a competition of CO and O_2 for adsorption sites.

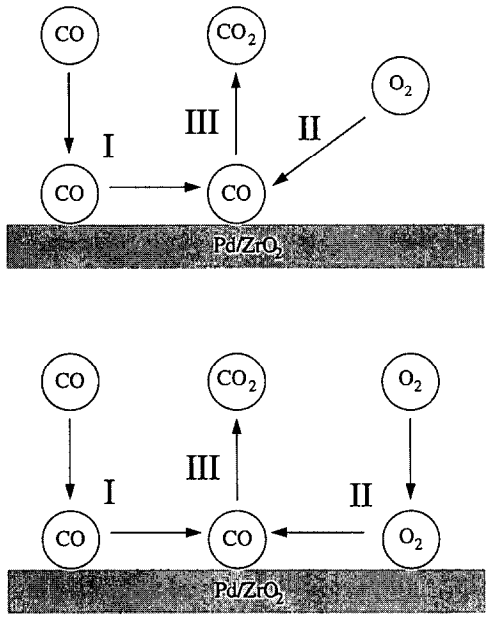

Fig. 12. Schematic representation of the Eley–Rideal (upper scheme) and Langmuir–Hinshelwood (lower scheme) reaction mechanisms.

At high p_{CO} values the surface is covered by adsorbed CO, and the oxidation rate is limited by the number of adsorption sites available for O_2. Lowering the CO concentration increases the number of accessible O_2 adsorption sites and leads to an increase in CO_2 production. Therefore, we conclude that the CO oxidation over a palladium/zirconia catalyst obtained from an amorphous $Pd_{25}Zr_{75}$ precursor is dominated by the Langmuir–Hinshelwood mechanism.

In the oscillating region, ϕ exhibits a dependence on modulation frequency ω_{CO} at constant temperature, T, and partial pressure ratio p_{CO}/p_{O_2}. Using the model of forced vibrations of a damped harmonic oscillator for describing $\phi(\omega_{CO})$ yields a characteristic eigenfrequency of the system for a defined set of experimental conditions. With a decreasing partial pressure ratio p_{CO}/p_{O_2} the eigenfrequency increases from $\omega_0 = 4.3 \times 10^{-3}$ Hz ($p_{CO}/p_{O_2} = 4 \times 10^{-3}$; $T = 180$°C) to $\omega_0 > 5 \times 10^{-2}$ Hz ($p_{CO}/p_{O_2} = 1 \times 10^{-4}$; $T = 180$°C). This points to an increasing reaction rate with decreasing partial pressure ratio due to the fact that the system is approaching the linear reaction regime.

In contrast to the observation that ϕ never reaches zero in experiments employing a modulation of the CO inlet concentration, we consistently detect $\phi = 0$ when varying the O_2 partial pressure *for all experimental conditions*. Obviously, the CO_2 production follows immediately (within experimental limits) any change in the O_2 concentration. Therefore, we conclude that the process of adsorption followed by surface movement of CO to the actual reaction site determines the rate of the CO oxidation (Fig. 12, I).

5. Conclusions

Analysing time dependent IR spectra of product and unconverted reactant of the CO oxidation over a $Pd_{25}Zr_{75}$ catalyst obtained as a function of the external perturbation allows discrimination of parameter regimes characterized by different reaction orders. Examination of the phase shift values excludes an Eley–Rideal mechanism, and provides hints on the rate limiting step of the Langmuir–Hinshelwood mechanism for CO oxidation. The process of adsorption and surface movement of CO to the actual reaction site determines the rate of the CO oxidation on a palladium/zirconia catalyst prepared using an amorphous $Pd_{25}Zr_{75}$ precursor.

Application of modulation spectroscopy in terms of varying the inlet mass flow of the reactant gases to the study of heterogenous catalyzed reactions is a straightforward method to examine mechanistic and kinetic aspects of possible reaction paths. Based on this investigation we will expand the technique to the study of catalyst surfaces by diffuse reflectance spectroscopy. Detection of signal variations of surface bound species when introducing an external perturbation to the system and application of the formalism of two-dimensional IR-spectroscopy will give further insight to reaction paths and kinetics of intermediates.

Acknowledgements

The authors thank A. Baiker for stimulating discussions, and for making the Pd/Zirconia sample available. We are indebted to R. Willi for valuable advice in the design of the IR detection system. We are grateful to D. Franzke, R. Hugi, R. Köppel, Th. Kunz and J. Weigel for their help with various aspects of this work.

References

[1] D. Böcker and E. Wicke, Ber. Bunsenges. Phys. Chem. 89 (1985) 629.
[2] B.C. Sales, J.E. Turner and M.B. Maple, Surf. Sci. 114 (1982) 381.
[3] T. Engel and G. Ertl, Adv. Catal. 28 (1979) 1.
[4] H. Conrad, G. Ertl and J. Küppers, Surf. Sci. 76 (1978) 323.
[5] T. Engel and G. Ertl, J. Chem. Phys. 69 (1978) 1267.
[6] T. Engel, J. Chem. Phys. 69 (1978) 373.
[7] S. Ladas, R. Imbihl and G. Ertl, Surf. Sci. 219 (1989) 88.
[8] Y.Q. Deng, T.G. Nevell and M.G. Jones, Catal. Lett. 34 (1995) 313.
[9] A. Palazov, G. Kadinov, C. Bonev, R. Dimitrova and D. Shopov, Surf. Sci. 225 (1990) 21.
[10] T. Ioannides, A.M. Efstathiou, Z.L. Zhang and X.E. Verykios, J. Catal. 156 (1995) 265.
[11] E. Gulari, X. Zhou and C. Sze, Catal. Today 25 (1995) 145.
[12] A. Baiker, D. Gasset, J. Lenzner, A. Reller and R. Schögl, J. Catal. 126 (1990) 555.
[13] A. Baiker, M. Maciejewski and S. Tagliaferd, Ber. Bunsenges. Phys. Chem. 97 (1993) 3.
[14] P. Bamickel, A. Wokaun and A. Baiker, J. Chem. Soc., Faraday Trans. 87 (2) (1991) 333.
[15] I. Noda, J. Am. Chem. Soc. 111 (1989) 8116.
[16] I. Noda, Appl. Spectrosc. 44 (1990) 550.
[17] I. Noda, A.E. Dowrey and C. Marcott, Appl. Spectrosc. 47 (1993) 1317.
[18] H.J. Güntherodt, in: S. Steeb and H. Warlimont (Eds.), Rapidly Quenched Metals, Vol. II (Elsevier, Amsterdam, 1985) p. 1591.
[19] J. De Pietro, PhD Thesis (No. 8936), Swiss Federal Institute of Technology, ETH, Zürich, 1989.
[20] D. Gasser and A. Baiker, Appl. Catal. 48 (1989) 279.